

Switchable Reconfiguration of an Interlocked DNA Olympiadane Nanostructure**

Chun-Hua Lu, Xiu-Juan Qi, Alessandro Cecconello, Stefan-Sven Jester, Michael Famulok, and Itamar Willner*

Abstract: Interlocked DNA rings (catenanes) are interesting reconfigurable nanostructures. The synthesis of catenanes with more than two rings is, however, hampered, owing to low yields of these systems. We report a new method for the synthesis of catenanes with a controlled number of rings in satisfactory yields. Our approach is exemplified by the synthesis of a five-ring DNA catenane that exists in four different configurations. By the use of nucleic acids as “fuels” and “antifuels”, the cyclic reconfiguration of the system across four states is demonstrated. One of the states, olympiadane, corresponds to the symbol of the Olympic Games. The five-ring catenane was implemented as a mechanical scaffold for the reconfiguration of Au NPs. The advantages of DNA catenanes over supramolecular catenanes include the possibility of generating highly populated defined states and the feasibility of tethering nanoobjects to the catenanes, which act as a mechanical scaffold to reconfigure the nanoobjects.

The base sequence in DNA encodes substantial structural and functional information in the biopolymer. This encoded information provides the basis for the development of the area of DNA nanotechnology and has been extensively used for the assembly of one-,^[1] two-,^[2] and three-dimensional^[3] nanostructures, for designing DNA machines,^[4] for the application of DNA as a scaffold for programmed synthesis^[5] and as a functional nanocontainer and carrier material,^[6] and

for stimulating directional electron-transfer cascades.^[7] An interesting family of DNA nanostructures consists of interlocked DNA rings—catenanes. DNA catenanes were identified in nature,^[8] and different reports addressed the man-made synthesis of two-ring^[9] or three-ring catenanes.^[10] Besides the structural characterization of DNA catenanes, their use as functional DNA machines was reported, and the switchable programmed reconfiguration of catenated DNAs by the use of nucleic acids,^[11] variable pH values, or the combination of a metal ion and a ligand^[12] as fuels and antifuels was demonstrated.

Supramolecular catenane structures have been the subject of extensive research in the past two decades, and ingenious methods to construct catenanes based on transition-metal complexes or donor–acceptor pairs have been reported.^[13] Different external triggers, such as pH,^[14] redox^[15] or photonic^[16] stimuli, were applied to reconfigure the supramolecular catenanes. Despite the impressive progress in developing supramolecular catenanes, the development of DNA-based catenanes may reveal several advantages: 1) The transitions between reconfigured states in supramolecular structures are often based on weak electrostatic or donor–acceptor interactions, thus leading to a mixture of the states. In contrast, the duplex stability of reconfigured DNA catenane structures can be tuned, thus leading to highly populated states. 2) The synthesis of supramolecular catenanes of enhanced complexity, beyond [2]catenanes, proceeds in low yields, and the stimuli-controlled reconfiguration of these structures is difficult. In contrast, the availability of different triggers to reconfigure DNA nanostructures, such as strand displacement,^[17] pH (i-motif),^[18] metal ions (T–Hg²⁺–T; C–Ag⁺–C),^[19] G-quadruplexes,^[20] and light,^[21] paves the way for the design of distinct multistate, catenated nanostructures. 3) The tethering of molecular or macromolecular objects to supramolecular catenanes, and the use of the molecular machines as a means to reconfigure the objects, is an unresolved challenge. In contrast, the tethering of molecular, macromolecular, and nanoparticle objects to the DNA catenanes is feasible by the hybridization of nucleic acid functionalized objects onto the DNA scaffold. Indeed, the reconfiguration of Au nanoparticles (NPs) and of Au NP/fluorophore conjugates by means of a three-ring catenane was reported previously, and control over the plasmonic properties of the resulting nanostructure was demonstrated.^[11]

The development of interlocked DNA catenanes suffers, however, from several limitations. To date, only the synthesis of two-ring or three-ring catenanes has been reported. The preparation of DNA catenanes of higher complexity (five rings or more) is, at present, impossible owing to low yields.

[*] Dr. C. H. Lu, X. J. Qi, A. Cecconello, Prof. I. Willner
Institute of Chemistry and The Center for Nanoscience and
Nanotechnology, The Hebrew University of Jerusalem
Jerusalem 91904 (Israel)
E-mail: willnea@vms.huji.ac.il

X. J. Qi

The Key Laboratory of Analysis and Detection Technology for Food
Safety of the MOE, College of Chemistry, Fuzhou University
Fuzhou 350002 (China)

Dr. S.-S. Jester

Kekulé Institut für Organische Chemie und Biochemie
University of Bonn
Gerhard-Domagk-Strasse 1, 53121 Bonn (Germany)

Prof. M. Famulok

LIMES Program Unit Chemical Biology and Medicinal Chemistry
c/o Kekulé Institut für Organische Chemie und Biochemie
University of Bonn
Gerhard-Domagk-Strasse 1, 53121 Bonn (Germany)

[**] This research is supported by the MULTI project (No. 317707) of the
EC Seventh Framework Programme. The study was performed
under the auspices of the MINERVA Center for Biohybrid Complex
Systems.



Supporting information for this article is available on the WWW
under <http://dx.doi.org/10.1002/anie.201403202>.

The synthesis of multiring catenanes is not only an artistic challenge, but multiring catenanes should exhibit programmed reconfiguration across many states. Herein we report a novel, versatile synthetic approach to DNA catenanes consisting of a predefined number of DNA rings. As an example, we present the synthesis of a five-ring DNA catenane. We discuss the mechanical, switchable, and reversible reconfiguration of the five-ring catenane across four different states, including the assembly of the “DNA olympiadane” (Olympic Games symbol) as one of the states. We present the single-molecule imaging of the olympiadane nanostructure and the use of the catenated five-ring DNA as a device for the programmed assembly of different arrangements of Au nanoparticles. Although a supramolecular interlocked donor–acceptor five-ring olympiadane catenane was reported previously,^[22] its reconfiguration into different isomers was impossible.

The synthesis of the five-ring catenane is schematically displayed in Figure 1. In the first step, the two interhybridized single-stranded duplexes L_1/L_2 and L_4/L_5 were capped with strands $C_1 + C_2$ and $C_4 + C_5$, respectively, and the resulting systems were ligated and purified to form the interlocked two-

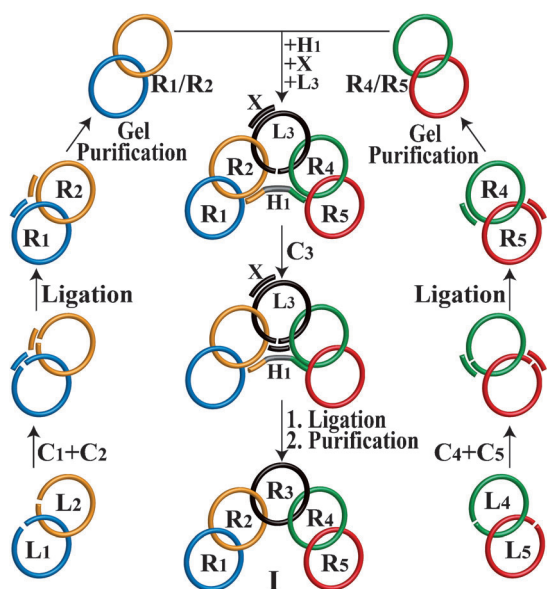


Figure 1. Synthesis and purification of the five-ring catenane in state I.

ring catenanes R_1/R_2 and R_4/R_5 , respectively. The two-ring catenanes R_1/R_2 and R_4/R_5 were then treated with the “helper” nucleic acid H_1 and the single-stranded nucleic acid L_3 , which hybridized with the respective sequences of rings R_2 and R_4 . A short strand X was hybridized with the single-stranded nucleic acid L_3 . The “helper” unit H_1 is partially complementary to rings R_2 and R_4 and functions as a bridge to concentrate the two-ring nanostructures R_1/R_2 and R_4/R_5 into a favorable configuration for the threading of L_3 through R_2 and R_4 . Subsequently, the interthreaded strand L_3 was capped with C_3 and ligated. Finally, the resulting supramolecular five-ring structure in configuration I was purified by electrophoresis, during which the H_1 , X , and C_3

units were removed from the structure (for details of the electrophoretic separation of the five-ring catenated structure, see Figure S1 in the Supporting Information). The incorporation of the “helper” unit H_1 and the single-stranded unit X , as functional components in the synthesis of the five-ring catenane in configuration I, is essential for the preparation of this nanostructure in high yields. Whereas the strand H_1 concentrates the rings R_1/R_2 and R_4/R_5 for the effective interthreading of strand L_3 , strand X rigidifies strand L_3 into a quasicircular structure that prevents the formation of L_3 oligomers and their interthreading and subsequent ligation with the R_1/R_2 and R_4/R_5 rings (for details of the specific functions of the H_1 and X units, see Figure S2). The yield for the generation of the R_1/R_2 and R_4/R_5 subunits was 24 and 28%, respectively. The yield, after purification and separation, for the preparation of the five-ring nanostructure from the two-ring subunits was estimated to be approximately 27%. The isolated purified five-ring nanostructure revealed the appropriate mass (calcd: m/z 133948.6; found: 134041.2; for details, see Figure S3 and Table S1).

The dynamic reconfiguration of the five-ring catenane is displayed in Figure 2a. The five-ring catenane consisting of rings R_1 – R_5 was initially set in the configuration corresponding to state I, in which the strands F_1 and F_2 were partially hybridized with the respective domains X_1 and X_2 associated with rings R_2 and R_4 . Rings R_1 and R_5 were hybridized with rings R_2 and R_4 through hybridization of the sequences X_3/X_3' and X_4/X_4' , respectively. The five-ring catenane was functionalized with two fluorophore-modified strands: a Cy3-modified strand associated with R_1 and a Cy5.5-modified strand linked to R_5 . Also, two quencher-modified strands (one with the quencher BHQ2 and one with IABRQ) were hybridized with the ring R_3 . The two fluorophore- and two quencher-modified units acted as functional optical labels for probing the states of the device. Treatment of the five-ring catenane in state I with the antifuel strand aF_2 and the fuel strand F_4 resulted in the strand displacement and release of ring R_5 through the removal of F_2 by the formation of a stabilized F_2/aF_2 duplex, and the reconfiguration of state I to state II, in which ring R_5 binds to domain X_2 of R_4 . In this configuration, the Cy5.5 fluorophore associated with R_5 is in close proximity to the quencher IABRQ, thus leading to its quenching, whereas the fluorescence of Cy3 is unaffected. The treatment of state II with F_2 and aF_4 reconfigured the system into state I. Similarly, the treatment of state I with a F_3 strand and an aF_1 strand resulted in the displacement of ring R_1 from the sequence X_3 associated with ring R_2 and the removal of strand F_1 by the formation of the duplex F_1/aF_1 . This set of reactions resulted in the transition of ring R_1 to the domain X_1 associated with ring R_2 to yield state III. In this configuration, the short distance separating Cy3 from the quencher unit BHQ2 linked to ring R_3 led to the quenching of the Cy3 fluorophore. The treatment of state III with F_1 and aF_3 restored state I.

Figure 2a maps all possible switchable and reversible transitions of the five-ring catenane system. For example, the treatment of state II with strands F_3 and aF_1 leads to the “olympiadane” configuration, state IV. Similarly, when state III is exposed to F_4 and aF_2 , the same “olympiadane”

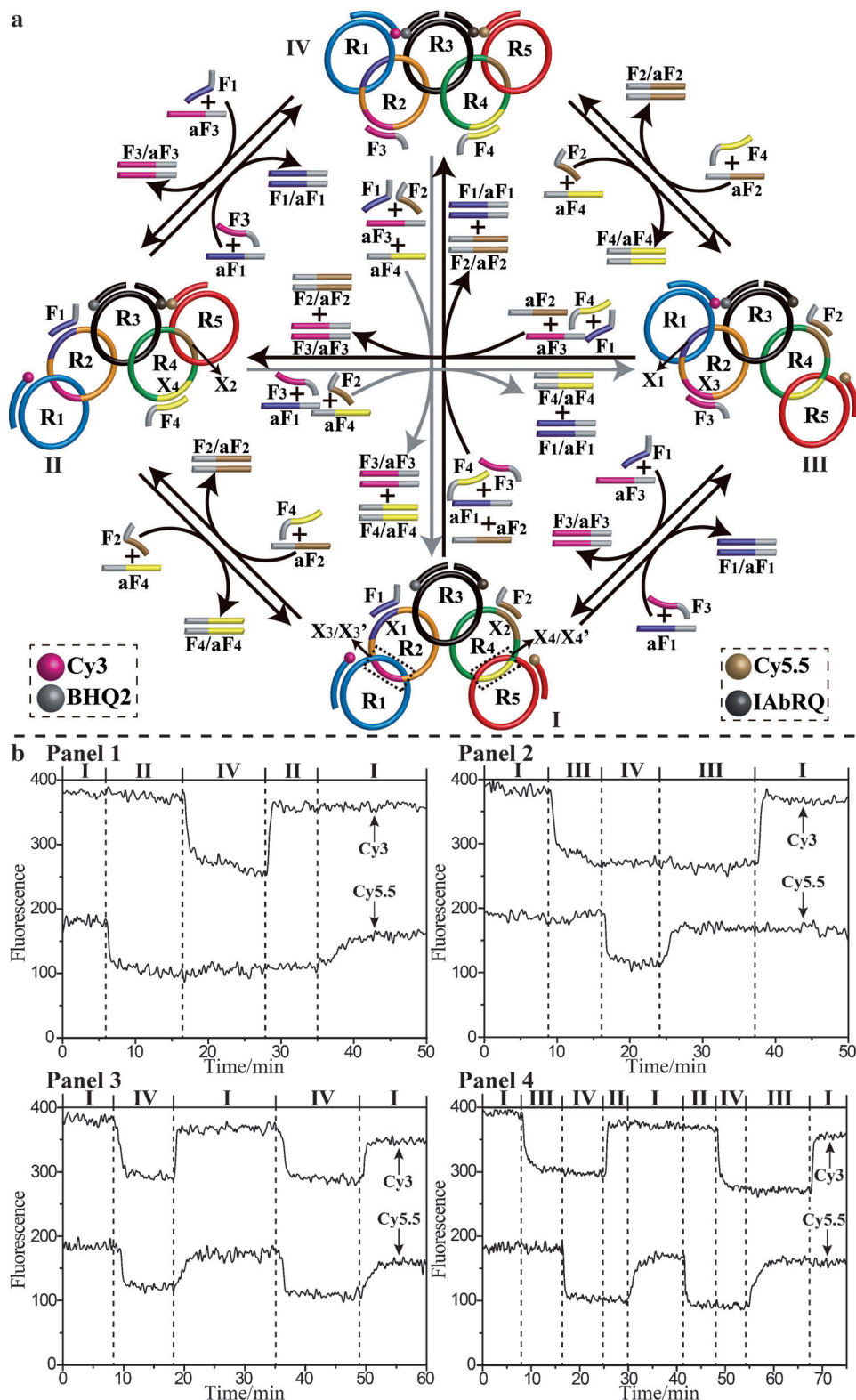


Figure 2. Monitoring by fluorescence of the switchable reconfiguration of the five-ring catenane system. a) Cyclic reconfiguration of the system across states I–IV by the use of appropriate fuel and antifuel strands. The catenane is labeled with the two fluorophores Cy3 and Cy5.5 and the two quencher units BHQ2 and IAbRQ. The fluorescence intensities of the fluorophores are used to identify structural transitions between the states. b) Fluorescence changes of the fluorophores Cy3 and Cy5.5 upon cyclic reconfiguration of the five-ring catenane through different paths. Panel 1: transition I→II→IV→II→I; panel 2: I→III→IV→III→I; panel 3: I→IV→I→IV→I; panel 4: I→III→IV→II→I→II→IV→III→I.

configuration is obtained. Alternatively, the treatment of state I with strands F_3 and F_4 as well as strands aF_1 and aF_2 leads directly to the “olympiadane” five-ring configuration. In the “olympiadane” nanostructure, fluorophores Cy3 and Cy5.5 are both in close proximity to the quencher units, BHQ2 and IAbRQ, thus leading to the quenching of the two fluorophores. Similarly, direct switchable transitions between states II and III proceed upon exposure of the states to the respective fuel (F) and antifuel (aF) strands.

Figure 2b displays the fluorescence changes upon the reversible transitions of the five-ring catenane across the different states. For example, in panel 1, the cyclic transitions of states I→II→IV→II→I is displayed. The formation of state II from I is accompanied by a decrease in the fluorescence of Cy5.5, whereas the fluorescence of Cy3 is almost unaffected. The reconfiguration of state II into IV is accompanied by a decrease in the fluorescence of Cy3, whereas the fluorescence of Cy5.5 is unaffected. Upon the stepwise restoration of state I from state IV, the fluorophores show the expected fluorescence changes. For a detailed discussion of the fluorescence changes associated with the stimuli-triggered transitions shown in panels 2–4 of Figure 2b as well as the fluorescence changes corresponding to the transitions between states II and III, see Figure S4 in the Supporting Information and accompanying discussions.

The formation of the olympiadane five-ring nanostructure was then imaged at the single-molecule level by atomic force microscopy. Figure 3b shows the AFM image of a large area containing “olympiadane” nanostructures. Enlarged images (rectangular

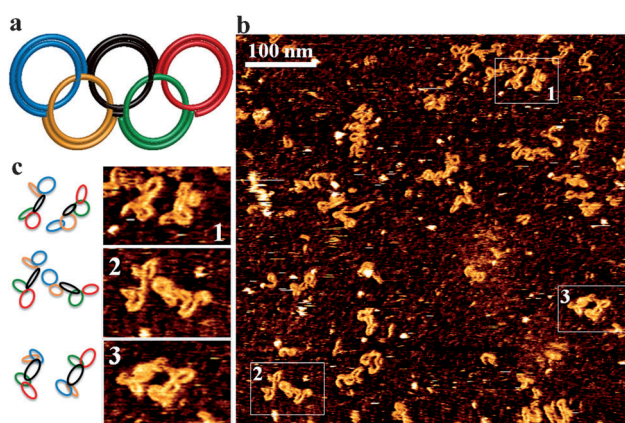


Figure 3. HyperDrive AFM images of the five-ring catenane in state IV. The catenane structure was rigidified by the hybridization of complementary nucleic acid strands to the rims of the rings. a) Schematic configuration of the interlocked five-ring catenane. b) Large-area image of the five-ring nanostructures. c) Enlarged domains of the image in (b) and corresponding schematic structural models of the five-ring catenane nanostructures observed by AFM.

areas labeled 1–3) are shown in Figure 3c, in which the schematic configuration of the observed olympiadane five-ring nanostructures are shown adjacent to the experimental images. In all of these nanostructures, five interlocked rings consistent with state IV are observed. The AFM images of the sample show footprint sizes of about $65 \times 20 \text{ nm}^2$, for example, for the smallest rectangles drawn around the five-ring catenanes. The individual DNA macrocycles have diameters in the range of 10–15 nm, consistent with the design of base pairs per ring (for the precise number and composition of bases comprising the different rings and further discussion related to the images, see Table S2 and Figure S5).

The fueled transitions of the interlocked five-ring catenane system were then implemented as a molecular mechanical device for the programmed switchable organization of Au NPs. Au NPs with a diameter of 5 nm were functionalized with dithiolated nucleic acids **1** and **2**, which are complementary to sequences X_5 and X_6 associated with the rims of rings R_1 and R_5 . Similarly, NPs with a diameter of 15 nm were modified with a single nucleic acid **3** complementary to sequence X_7 , which is part of the rim of ring R_3 . Figure 4a (left) shows the assembly of Au NP nanostructures formed upon the hybridization of two 5 nm Au NPs and one 15 nm Au NP to state I of the five-ring catenane. STEM images of the resulting Au NPs associated with the five-ring catenane in state I show that the nanoparticles are spatially separated with characteristic separation distances of $d_1 \approx 14.5 \text{ nm}$; $d_2 \approx 25 \text{ nm}$; $d_3 \approx 32 \text{ nm}$ (Figure 4b; for large-area images of the NP structures, see Figure S6; for histograms of the different separation distances d_1 , d_2 , and d_3 , see Figure S7). The treatment of state I functionalized with the three Au NPs with fuel strands F_3 and F_4 and antifuel strands aF_1 and aF_2 yielded a functionalized olympiadane nanostructure modified with the three Au NPs (Figure 4a, right). The transition of state I functionalized with three Au NPs to functionalized state IV yielded a compact assembly of the Au NPs (Figure 4c). The

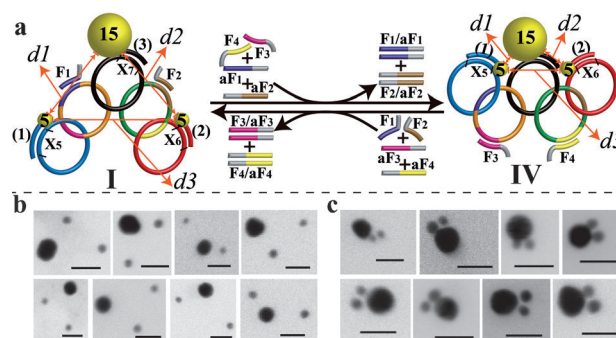


Figure 4. Programmed assembly of Au NPs by the five-ring catenane system. a) Modification of the five-ring catenane in state I with two 5 nm Au NPs and one 15 nm Au NP, and cyclic reconfiguration of the Au NP assembly by means of the DNA machinery between states IV and I. b) Representative STEM images of the Au NPs associated with state I (scale bars: 20 nm). c) Representative STEM images of the Au NPs associated with state IV (scale bars: 20 nm).

corresponding separation distances are $d_1 \approx 0.75 \text{ nm}$; $d_2 \approx 1.5 \text{ nm}$; $d_3 \approx 2 \text{ nm}$ (for large-area images of the resulting nanostructures and the respective histograms of the distances separating the NPs, see Figures S8 and S9). The yield for the transformation of the state I gold-nanoparticle-modified nanostructure into the state IV gold-nanoparticle-modified nanostructure was estimated to be approximately 80%. Further treatment of functionalized state IV with fuel strands F_1 and F_2 and antifuel strands aF_3 and aF_4 regenerated the functionalized state I, thus revealing the cyclic reconfiguration of the NPs.

In summary, the present study has introduced a paradigm for the synthesis of polymeric interlocked catenated rings that included a controlled number of rings in their structure. The interlocking process leads to functional nanometer-sized macromolecular assemblies. The systems may find important future application as promising devices for molecular logic operations and add new dimensions to the area of DNA nanotechnology. The study demonstrated the cyclic reconfiguration of the interlocked rings across four defined states. By increasing the number of interlocked rings, the number of transitions and reconfigured states may be increased, thus enabling the construction of memory systems. Furthermore, the ring structure of the catenane suggests that these systems will be resistant to hydrolytic cleavage by enzymes (for example, Exo I, Exo III), a feature that may be useful for the construction of intracellular sensing devices and the control of intracellular processes. For example, the fluorescence imaging of two different microRNAs by the reconfiguration of the fluorophore/quencher-functionalized catenated machinery may be envisaged. Also, since many viruses or eukaryotic mitochondria possess circular genes, the catenated system, and its dictated reconfiguration, may act as an artificial cell vector for the programmed transcription and controlled synthesis of proteins.

Received: March 11, 2014

Published online: May 30, 2014

Keywords: DNA catenanes · molecular devices · nanoparticles · strand displacement · switches

- [1] a) Y. Liu, C. Lin, H. Li, H. Yan, *Angew. Chem.* **2005**, *117*, 4407–4412; *Angew. Chem. Int. Ed.* **2005**, *44*, 4333–4338; b) Y. Weizmann, A. B. Braunschweig, O. I. Wilner, Z. Cheglakov, I. Willner, *Proc. Natl. Acad. Sci. USA* **2008**, *105*, 5289–5294.
- [2] a) E. Winfree, L. Furong, L. A. Wenzler, N. C. Seeman, *Nature* **1998**, *394*, 539–544; b) C. Mao, W. Sun, N. C. Seeman, *J. Am. Chem. Soc.* **1999**, *121*, 5437–5443; c) T. H. LaBean, H. Yan, J. Kopatsch, F. Liu, E. Winfree, J. H. Reif, N. C. Seeman, *J. Am. Chem. Soc.* **2000**, *122*, 1848–1860.
- [3] a) Y. He, T. Ye, M. Su, C. Zhang, A. E. Ribbe, W. Jiang, C. Mao, *Nature* **2008**, *452*, 198–201; b) J. Chen, N. C. Seeman, *Nature* **1991**, *350*, 631–633; c) H. Dietz, S. M. Douglas, W. M. Shih, *Science* **2009**, *325*, 725–730.
- [4] a) M. K. Beissenhirtz, I. Willner, *Org. Biomol. Chem.* **2006**, *4*, 3392–3401; b) J. Bath, A. J. Turberfield, *Nat. Nanotechnol.* **2007**, *2*, 275–284; c) Y. Krishnan, F. C. Simmel, *Angew. Chem.* **2011**, *123*, 3180–3215; *Angew. Chem. Int. Ed.* **2011**, *50*, 3124–3156.
- [5] a) O. I. Wilner, Y. Weizmann, R. Gill, O. Lioubashevski, R. Freeman, I. Willner, *Nat. Nanotechnol.* **2009**, *4*, 249–254; b) J. Fu, M. Liu, Y. Liu, N. W. Woodbury, H. Yan, *J. Am. Chem. Soc.* **2012**, *134*, 5516–5519.
- [6] E. S. Andersen, M. Dong, M. M. Nielsen, K. Jahn, R. Subramani, W. Mamdouh, M. M. Golas, B. Sander, H. Stark, C. L. Oliveira, J. S. Pedersen, V. Birkedal, F. Besenbacher, K. V. Gothelf, J. Kjems, *Nature* **2009**, *459*, 73–76.
- [7] G. Piperberg, O. I. Wilner, O. Yehezekeli, R. Tel-Vered, I. Willner, *J. Am. Chem. Soc.* **2009**, *131*, 8724–8725.
- [8] B. Hudson, J. Vinograd, *Nature* **1967**, *216*, 647–652.
- [9] a) Y. Liu, A. Kuzuya, R. Sha, J. Guillaume, R. Wang, J. W. Canary, N. C. Seeman, *J. Am. Chem. Soc.* **2008**, *130*, 10882–10883; b) D. Han, S. Pal, Y. Liu, H. Yan, *Nat. Nanotechnol.* **2010**, *5*, 712–717; c) T. L. Schmidt, A. Heckel, *Nano Lett.* **2011**, *11*, 1739–1742.
- [10] J. Elbaz, Z. G. Wang, F. Wang, I. Willner, *Angew. Chem.* **2012**, *124*, 2399–2403; *Angew. Chem. Int. Ed.* **2012**, *51*, 2349–2353.
- [11] J. Elbaz, A. Cecconello, Z. Fan, A. O. Govorov, I. Willner, *Nat. Commun.* **2013**, *4*, 2000.
- [12] C. H. Lu, A. Cecconello, J. Elbaz, A. Credi, I. Willner, *Nano Lett.* **2013**, *13*, 2303–2308.
- [13] a) D. B. Amabilino, J. F. Stoddart, *Chem. Rev.* **1995**, *95*, 2725–2828; b) T. J. Hubin, D. H. Busch, *Coord. Chem. Rev.* **2000**, *200*, 5–52; c) V. Balzani, A. Credi, F. M. Raymo, J. F. Stoddart, *Angew. Chem.* **2000**, *112*, 3484–3530; *Angew. Chem. Int. Ed.* **2000**, *39*, 3348–3391; d) B. Champin, P. Mobian, J. P. Sauvage, *Chem. Soc. Rev.* **2007**, *36*, 358–366; e) J. A. Faiz, V. Heitz, J. P. Sauvage, *Chem. Soc. Rev.* **2009**, *38*, 422–442.
- [14] a) X. Yan, P. Wei, Z. Li, B. Zheng, S. Dong, F. Huang, Q. Zhou, *Chem. Commun.* **2013**, *49*, 2512–2514; b) P. R. Ashton, V. Balzani, V. Balzani, A. Credi, H. D. Hoffmann, M. V. Martínez-Díaz, F. M. Raymo, J. F. Stoddart, M. Venturi, *Chem. Eur. J.* **2011**, *17*, 3482–3493.
- [15] a) M. B. Nielsen, C. Lomholt, J. Becher, *Chem. Soc. Rev.* **2000**, *29*, 153–164; b) D. Cao, M. Amelia, L. M. Klivansky, G. Koshkakarayan, S. I. Khan, M. Semeraro, S. Silvi, M. Venturi, A. Credi, Y. Liu, *J. Am. Chem. Soc.* **2010**, *132*, 1110–1122.
- [16] V. Balzani, A. Credi, M. Venturi, *Chem. Soc. Rev.* **2009**, *38*, 1542–1550.
- [17] a) B. Yurke, A. J. Turberfield, A. P. Mills, Jr., F. C. Simmel, J. L. Neumann, *Nature* **2000**, *406*, 605–608; b) Y. S. Shin, N. A. Pierce, *J. Am. Chem. Soc.* **2004**, *126*, 10834–10835.
- [18] a) K. Gehring, J. L. Leroy, M. Guéron, *Nature* **1993**, *363*, 561–565; b) D. Liu, S. Balasubramanian, *Angew. Chem.* **2003**, *115*, 5912–5914; *Angew. Chem. Int. Ed.* **2003**, *42*, 5734–5736; c) Z. G. Wang, J. Elbaz, F. Remacle, R. D. Levine, I. Willner, *Proc. Natl. Acad. Sci. USA* **2010**, *107*, 21996–22001.
- [19] a) Y. Miyake, H. Togashi, M. Tashiro, H. Yamaguchi, S. Oda, M. Kudo, Y. Tanaka, Y. Kondo, R. Sawa, T. Fujimoto, T. Machinami, A. Ono, *J. Am. Chem. Soc.* **2006**, *128*, 2172–2173; b) J. Elbaz, Z. G. Wang, R. Orbach, I. Willner, *Nano Lett.* **2009**, *9*, 4510–4514; c) Z. G. Wang, J. Elbaz, I. Willner, *Nano Lett.* **2010**, *11*, 304–309.
- [20] a) P. Alberti, J.-L. Mergny, *Proc. Natl. Acad. Sci. USA* **2003**, *100*, 1569–1573; b) J. T. Davis, G. P. Spada, *Chem. Soc. Rev.* **2007**, *36*, 296–313.
- [21] a) H. Asanuma, T. Ito, T. Yoshida, X. Liang, M. Komiyama, *Angew. Chem.* **1999**, *111*, 2547–2549; *Angew. Chem. Int. Ed.* **1999**, *38*, 2393–2395; b) H. Kang, H. Liu, J. A. Phillips, Z. Cao, Y. Kim, Y. Chen, Z. Yang, J. Li, W. Tan, *Nano Lett.* **2009**, *9*, 2690–2696; c) M. You, Y. Chen, X. Zhang, H. Liu, R. Wang, K. Wang, K. R. Williams, W. Tan, *Angew. Chem.* **2012**, *124*, 2507–2510; *Angew. Chem. Int. Ed.* **2012**, *51*, 2457–2460.
- [22] a) D. B. Amabilino, P. R. Ashton, A. S. Reder, N. Spencer, J. F. Stoddart, *Angew. Chem.* **1994**, *106*, 1316–1319; *Angew. Chem. Int. Ed. Engl.* **1994**, *33*, 1286–1290; b) D. B. Amabilino, P. R. Ashton, V. Balzani, S. E. Boyd, A. Credi, J. Y. Lee, S. Menzer, J. F. Stoddart, M. Venturi, D. J. Williams, *J. Am. Chem. Soc.* **1998**, *120*, 4295–4307.